Synthesis of Hierarchical Porous ZnO Disklike Nanostructures for Improved Photovoltaic Properties of Dye−Sensitized Solar Cells

ARTICLE *in* THE JOURNAL OF PHYSICAL CHEMISTRY C · JULY 2010

Impact Factor: 4.77 · DOI: 10.1021/jp100637c

9 AUTHORS, INCLUDING:

Jianxiong Wang
Nanyang Technological University
69 PUBLICATIONS **3,274** CITATIONS

SEE PROFILE

Lin-Bao Luo
Hefei University of Technology
112 PUBLICATIONS **2,623** CITATIONS

SEE PROFILE

S. T Lee
City University of Hong Kong
615 PUBLICATIONS **24,215** CITATIONS

SEE PROFILE

Synthesis of Hierarchical Porous ZnO Disklike Nanostructures for Improved Photovoltaic Properties of Dye-Sensitized Solar Cells

J. X. Wang, C. M. L. Wu,* W. S. Cheung, L. B. Luo, Z. B. He, G. D. Yuan, W. J. Zhang, C. S. Lee, and S. T. Lee

Department of Physics and Materials Science and Center of Super-Diamond and Advanced Films (COSDAF), City University of Hong Kong, Hong Kong SAR, People's Republic of China

Received: January 22, 2010; Revised Manuscript Received: June 25, 2010

We report on the synthesis of a porous hierarchical disklike ZnO nanostructure fabricated via a simple low-temperature hydrothermal method for photovoltaic applications. The hierarchical ZnO nanostructures consist of porous ZnO nanowires growing in six symmetric directions and form a disklike shape. Owing to the enlarged surface area and natural electron collection routes of the ZnO hierarchical nanostructures, dye-sensitized solar cells based on these structures exhibit improved photovoltaic performance compared with that of the ZnO nanowire arrays. Our results suggest that porous hierarchical nanomaterials are promising materials for applications in dye-sensitized solar cells.

1. Introduction

Dye-sensitized solar cells (DSSCs) are considered as one of the most promising candidates for solar energy conversion devices due to their cost-effective features over the silicon-based solar cells.[1−3] A key component in DSSCs is the photoanode, which utilizes metal oxide nanoparticle film to absorb dye molecules for effective light harvesting.[3−5] When the photoanode is exposed to sunlight, electrons in the oxides are excited to the conduction band and then collected by the back contact for current generation.[6−8] Meanwhile, the recombination of the photoexcited electron−hole pairs limits the performance of the DSSC.[9,10] Photoanodes using one-dimensional (1D) nanostructures have been considered as a viable solution because they are able to provide a direct pathway for rapid collection of the photoexcited electrons and thus suppress the charge recombination process. Recently, better performance DSSCs employing 1D nanostructures, such as TiO_2 and ZnO nanowires/nanotubes, have been reported. The nanowire/nanotube-based DSSCs have been demonstrated to possess a faster electron collection with greater material flexibility than nanocrystalline films.[11−14] However, compared with DSSCs that use nanoparticles, 1D nanowires and nanotubes have a relatively lower specific surface area, which greatly reduces the dye loading of the photoanode and thus leads to a lower efficiency.[15−18] Therefore, the utilization of 1D nanostructures with high aspect ratios is preferred to overcome this problem. Among various kinds of 1D nanostructures that have been reported in recent years, porous hierarchical 1D nanostructures are of great interest for functional nanodevices because they offer a better electron collection while maintaining a large specific surface area for dye loading.[19−21] However, large-scale synthesis of porous hierarchical nanostructures at low temperatures remains a challenge, which limits their wide application in DSSCs.

In this paper, we report the synthesis of hierarchical ZnO nanostructured films and their applications as photoanodes in DSSCs. The hierarchical ZnO nanostructures consist of porous ZnO nanowires growing in six directions to form disklike shapes. These structures have advantages over conventional nanowire arrays in both light absorption and electron collection, and the photovoltaic properties of the DSSCs based on these structures can be remarkably improved.

2. Experimental Details

The hierarchical ZnO nanostructures were synthesized via a simple low-temperature hydrothermal method.[22,23] In brief, 20 mL of 0.1 M $ZnCl_2$ and 0.1 M hexamethylenamine aqueous solutions were mixed in an autoclaved container and kept at 50−80 °C for 10 min. A 40 mL mixed solution of 0.1 M $Zn(CH_3COOH)_2$ and hexamethylenetetramine (volume ratio = 1:1) was then added into the container. The pH value of the mixed solution was adjusted to 6−7 using a small quantity of ammonia solution. The solution was kept at 95 °C for 10 h, and a silicon (100) substrate (2 cm × 2 cm) was used to collect the hierarchical ZnO nanostructures. After the reaction, white powder can be found on the silicon substrate. The as-prepared product was then rinsed with deionized water several times and dried for morphology and structure characterizations.

To fabricate DSSCs, 0.5 g of hierarchical ZnO nanostructures was scratched off from the silicon substrate and mixed with 10 mL of diluted ethanol solution (DI water/ethanol was 1:1 in vol). After stirring for 15 min, 0.2 g of carbowax 1540 was added to the ethanol solution to form a sticky paste. The paste was then coated onto a F-doped tin oxide (FTO) glass substrate, and a uniform hierarchical nanostructure film was prepared by a conventional blade method. The ZnO nanostructure film was then sintered at 450 °C for 30 min in a furnace to produce a dense ZnO film with a thickness around 20 μm.

The as-prepared ZnO nanostructure film was soaked in ethanol solution with 0.5 mM $(Bu_4N)_2Ru(dcbpyH)_2(NCS)_2$ (commercially known as N719 dye) for 5 h to absorb dye molecules. After that, the sensitized ZnO film was rinsed in acetone to remove excessive dye molecules and dried with a flow of N_2. FTO glass with a thin Pt catalyst film was used as the counter electrode. The ZnO film electrode and the counter electrode were then sealed by a 60 μm thick hot-melt spacer, and the space was filled with liquid electrolyte (0.5 M LiI, 50

* To whom correspondence should be addressed. E-mail: apcmlwu@cityu.edu.hk.

10.1021/jp100637c
Published on Web 07/19/2010

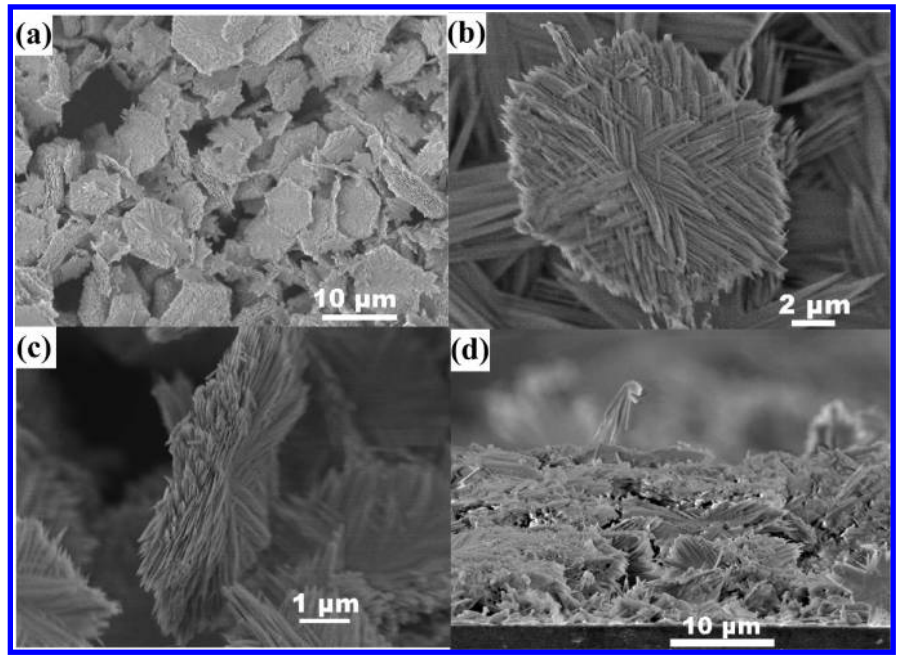

Figure 1. SEM images of the hierarchical ZnO nanostructures. (a) Top-view and (b) higher-magnification SEM image. (c) Side-view and (d) cross-sectional image of the photoanode based on the hierarchical ZnO nanostructures.

mM I_2, 0.5 M 4-tertbutylpyridine in 3-methoxypropionitrile). The active area of the DSSC is 0.22 cm^2. The DSSC was characterized with an Oriel solar simulated system (model 66902). The simulated sunlight intensity was AM 1.5G (100 mW/cm^2). Optical absorption spectra were measured by a UV−vis spectrophotometer (PE Lambda 750).

3. Results and Discussion

Figure 1a shows the typical scanning electron microscopy (SEM) image of the ZnO hierarchical nanostructures. It can be clearly seen that the ZnO hierarchical nanostructures are in a hexagonal disk shape with diameters in the range of 2−10 μm. Figure 1b presents the SEM image of one hierarchical disklike (HD) nanostructure at a higher magnification. The structures consist of dense nanowires growing in six directions. The thickness of the ZnO HD nanostructures is about 500 nm, which can be determined from the side-view SEM image, as shown in Figure 1c. Figure 1d shows a cross-sectional image of a ZnO HD film on an FTO-coated glass substrate after sintering. The thickness of the film was measured to be about 20 μm.

Transmission electron microscopy (TEM) was carried out to study the microstructure of the ZnO hierarchical disk. A typical image is shown in Figure 2a. It can be found that the HD nanostructure consists of nanowires growing in six symmetrical directions and the angle is about 60° between every two adjacent directions. Figure 2b shows a corresponding selected area electron diffraction (SAED) pattern of the ZnO HD nanostructures. The 6-fold symmetric distribution of diffraction spots in the pattern indicates that all nanowires contributing to the SAED pattern have the same crystallographic orientation. The zone axis of the SAED pattern is [0001], which is the *c* axis of the wurtzite ZnO, and the six symmetrical growth directions of the nanowires can be indexed to be $\pm[10\bar{1}0]$, $\pm[01\bar{1}0]$, and $\pm[1\bar{1}00]$. Figure 2c presents a higher-magnification TEM image of the ZnO nanowires taken from the edge of a ZnO HD nanostructure. As different from previously reported single-crystalline nanowires, the HD structures consist of highly porous nanowires. The pores are distributed uniformly throughout the nanowires and their diameters range from several nanometers to several tens

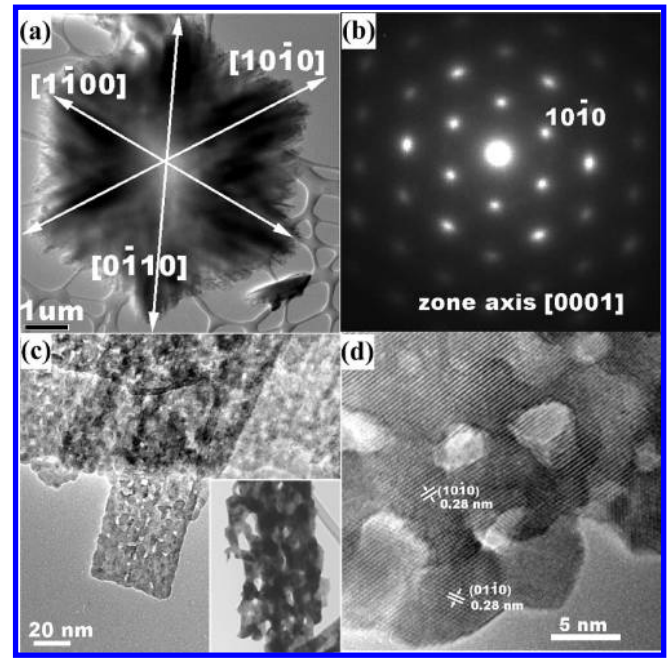

Figure 2. (a) Bright-field TEM image of the hierarchical disklike nanostructure. (b) SAED pattern of the nanowires in the hierarchical nanostructures. (c) Higher-magnification TEM image of the nanowires at the edge of the HD structure. The inset is the enlarged TEM image of a porous nanowire. (d) HRTEM image of a porous nanowire.

of nanometers, which can be observed from the enlarged TEM image shown in the inset of Figure 2c. Figure 2d shows a high-resolution TEM image of the porous nanowire. The two sets of fringes shown in this image correspond to the $(10\bar{1}0)$ and $(01\bar{1}0)$ planes of ZnO. These HRTEM results indicate that the porous nanowires have reserved their single-crystalline features.

Figure 3a−d shows a set of TEM images of the ZnO nanostructures found in the as-prepared ZnO HD sample, which clearly depict the evolution process of the ZnO HD nanostructures. Figure 3a presents a ZnO flower with the six symmetric arms, which provides the original framework for the formation of the ZnO HD structures. Subsequently, more nanowires can

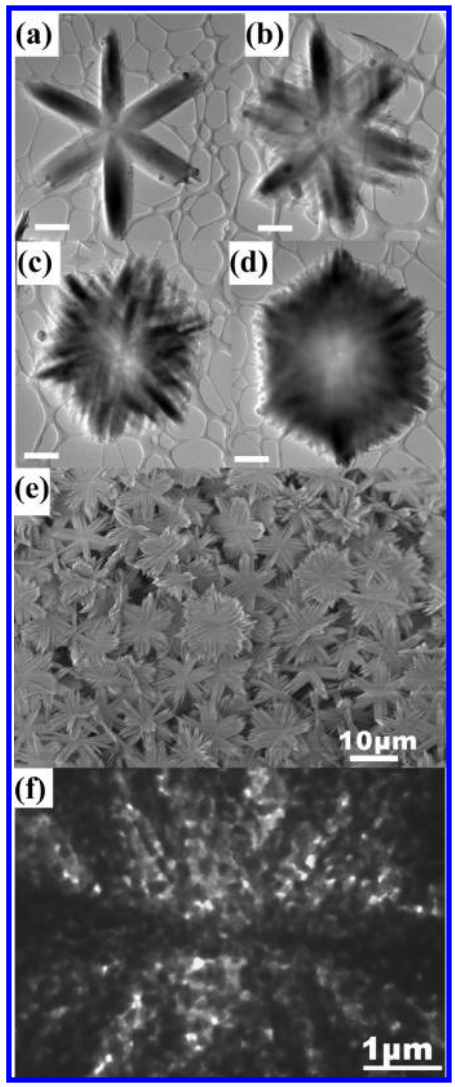

Figure 3. TEM images of the ZnO nanostructures (a−d) showing the evolution process of the hierarchical ZnO nanostructures. The scale bars are 1 μm. (e) Top-view SEM image of the as-prepared HD after growth for 1.5 h. Hexagonal HD ZnO nanostructures and nanoflowers with six symmetric arms can be clearly seen. (f) TEM image taken from the central region of the hierarchical nanostructures.

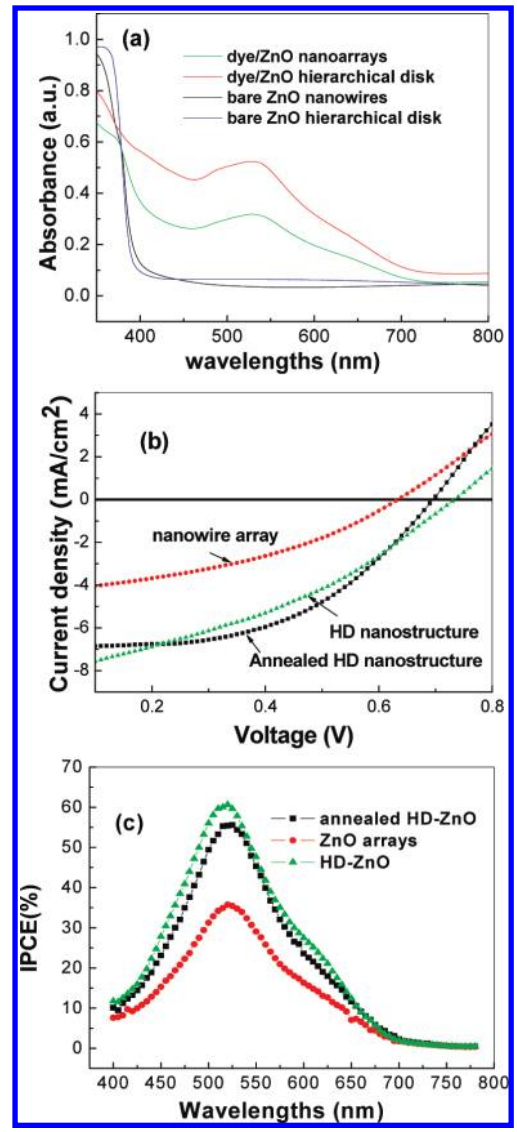

Figure 4. (a) Optical absorption spectra of the ZnO HD structured film and ZnO nanowire arrays sensitized with/without the dye. (b) Photocurrent density versus voltage characteristics of DSSCs based on the HD electrode and nanowire arrays. (c) Incident photon-to-current quantum efficiency (IPCE) of the DSSCs with ZnO HD and nanowire array electrodes.

grow on the ZnO flower (Figure 3b) to form the ZnO HD nanostructures (Figure 3c,d). This evolution process is also consistent with our SEM investigations: both the hexagonal ZnO HD nanostructures and the nanoflower with six symmetric arms can be found in the product collected during the synthesized process, as shown in Figure 3e. On the basis of the SEM and TEM investigations, we believe that the formation of the ZnO HD nanostructures undergoes a three-step process. The first step is the nucleation of small ZnO seeds in the solution, followed by the growth in six crystallographically equivalent directions to form the ZnO flowers. During the second step, these ZnO flowers serve as the frameworks for the continuous growth of new nanowires. During the final step, the formation of the disk-shaped structure occurs and it thickens along the *c* axis when more and more new nanowires are grown from existing ones. The formation of pores on the nanowires could be due to the aging effect of ZnO nanowires. The process is considered to be similar to the formation process of the tubular ZnO structures.[24−26] Because the ZnO synthesis reaction in solution is a reversible one, the precipitate of ZnO can be dissolved again at the appropriate pH value and reactant concentrations. As we know, a ZnO crystal is enclosed by the polarized (0001) plane and six nonpolarized planes. Compared with the six nonpolarized planes, the (0001) plane is unstable, and thus, the [0001] direction is the direction for fast dissolution. For ZnO HD nanostructures, because the nanowires grow in different ⟨110⟩ directions, their radial direction is the [0001] direction. Because of the thin radial thickness of the nanowires, the dissolution of ZnO along the [0001] directions can easily form small pores. It is worth noting that the pores are formed not only on the edge but also in the center of the ZnO HD nanostructures (Figure 3f), which will greatly increase the porosity of the hierarchical nanostructure film.

A dye-sensitized solar cell based on this porous HD nanostructure was fabricated. A photoanode using aligned ZnO nanowire arrays with the same thickness has also been fabricated as a control sample. The surface areas of the porous HD nanostructures and ZnO nanowire arrays are measured to be 21.8 and 12.3 $m^2\ g^{-1}$, respectively. Figure 4a shows the optical absorption spectra of the porous HD structures and nanowire arrays sensitized by the N719 dye. As a reference, the absorption

TABLE 1: Photovoltaic Properties of ZnO DSSCs

sample	J_{sc} [mA/cm^2]	V_{oc} [V]	FF [%][a]	η [%][a]	light intensity [mW/cm^2]
arrays	4.2	0.63	39.5	1.1	99.8
arrays	4.15	0.6	39.6	0.98	100.6
annealed arrays	3.98	0.64	41.8	1.06	100.4
annealed arrays	4.13	0.64	42.4	1.12	100.0
HD-ZnO	8.06	0.73	36.6	2.15	100.4
HD-ZnO	7.53	0.72	41.9	2.09	100.8
annealed HD-ZnO	6.92	0.69	52.5	2.49	100.6
annealed HD-ZnO	6.86	0.68	49.4	2.25	100.4

[a] The conversion efficiency, η, and fill factor, FF, are calculated from $\eta = P_{out,max}/P_{in}$ and FF $= P_{out,max}/(V_{oc} \times I_{sc})$, where $P_{out,max}$ is the maximum output power density and P_{in} is the incident light power density.

spectrum of ZnO HD nanostructures and ZnO nanowire arrays without dye modification are also presented. Without dye modification, no peaks in the visible range are found. The spectrum of the two dye-modified samples shows a peak centered around 530 nm, which corresponds to the intrinsic peak of the N719 dye absorbed on the ZnO surface. It can be seen that the spectrum of the dye/porous ZnO HD structures shows a higher intensity than that with the dye/ZnO nanowire arrays. This indicates that the porous ZnO HD structure absorbs more dye molecules and, therefore, can harvest more light than the ZnO nanowire array.

Figure 4b shows the photocurrent density (J) versus voltage (V) characteristics of the DSSCs based on the porous HD nanostructure and nanowire electrodes under air mass 1.5 global (AM 1.5G) illumination with an intensity of 100 mW/cm^2. Under the illumination of simulated sunlight, both the ZnO HD nanostructure and the nanowire solar cells yield obvious photocurrents. The fabricated DSSCs based on the HD nanostructures show a remarkably improved short-circuit photocurrent density (J_{sc}) and open-circuit voltage (V_{oc}). A J_{sc} of 8.0 mA/cm^2 and V_{oc} of 0.73 V for the best porous HD ZnO DSSC were obtained, compared with 4.2 mA/cm^2 and 0.63 V of the ZnO nanowire array DSSC. The fill factor (FF) and the overall efficiency (η) of the HD structure solar cell were calculated to be ~36.6% and ~2.1%, whereas the FF and η of the nanowire DSSC are 39.5% and 1.1%, respectively.

The performance of the HD-based DSSC can be further improved by annealing the porous HD nanostructures under H_2 at 350 °C for 5 h. The $J-V$ curve of the DSSC based on the annealed HD ZnO is shown in Figure 4b. It is worth mentioning that the J_{sc} decreased slightly to 6.9 mA/cm^2 after annealing. This may be due to the aggregation of the nanowires during annealing, which leads to a decrease of surface area. However, the FF of the annealed HD ZnO DSSC was remarkably improved compared with that of the nanowire DSSC. Normally, the FF of a ZnO solar cell is relatively low, ranging from 30 to 40% in our experiment. Without the annealing, the FF of the HD-ZnO structure DSSC is comparable to that of the ZnO nanowire DSSC. The FF of the HD-ZnO structure DSSC is 52.2% after annealing and is much larger than the FF of the ZnO nanowire array DSSC. Only a slight increase in FF was obtained for the ZnO nanowire DSSC after annealing. The detailed photovoltaic properties of the three kinds of DSSCs are tabulated in Table 1. The improvement in FF can be attributed to the reduction of the surface state and defects in the HD structures. Because the fabrication of the porous HD structure undergoes an aging process, the dissolution of ZnO to form the small pores leads to the formation of many defects

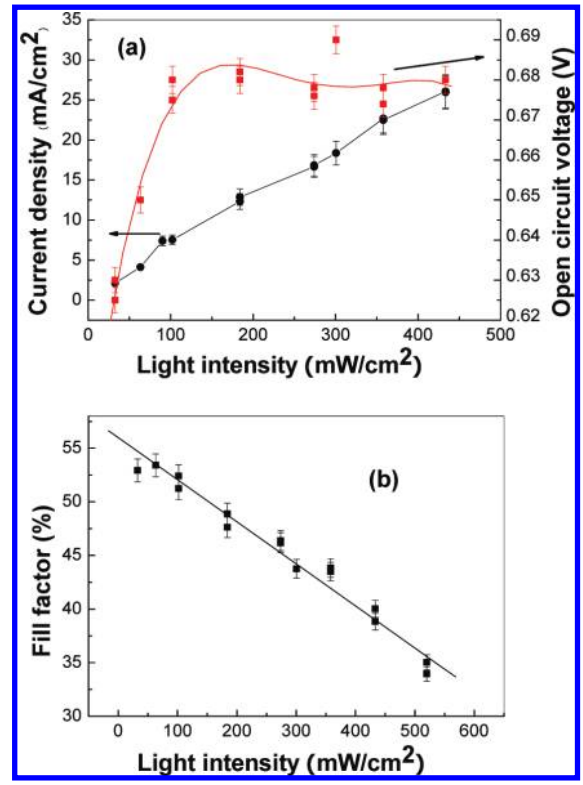

Figure 5. Photovoltaic properties of annealed HD DSSCs under different light intensities. (a) Short-current density (circle symbol) and open-circuit voltage (rectangular symbol) as functions of light intensity. (b) Fill factor as a function of light intensity.

on the surface of the HD structures. Because of the improvement in FF, an efficiency of 2.49% can be obtained for the DSSC based on the HD structures.

Furthermore, it can be found from Table 1 that all of the DSSCs based on the HD structures show improved photovoltaic properties, including J_{sc}, V_{oc}, and η. The average efficiency of the HD structure solar cell is about 2%. The efficiency of the HD-based DSSC is comparable to that of the ZnO nanoparticle DSSC[27] and is higher than most of the DSSCs using 1D ZnO nanostructures, such as ZnO nanowires, nanotubes, and nanoflowers.[11,18,21] It is worth noting that the efficiency of the porous ZnO HD solar cell is lower than that of TiO_2 nanoparticle based DSSCs. This may be due to several factors, including the low injection yield and low charge collection efficiency of the ZnO film. However, this concept of porous hierarchical nanowires may provide a route that can be applied to other electrode materials, such as TiO_2 and SnO_2, to fabricate the DSSCs with an improved performance.

The incident photocurrent conversion efficiency (IPCE) is shown in Figure 4c. The maximum efficiency of IPCE spectra shows the corresponding trend with the J_{sc} and η of each cell. The maximum efficiencies of the DSSC based on ZnO HD nanostructures with and without annealing are 55% and 60% at 520 nm, respectively, and both are higher than that of the nanowire DSSC (33%). The IPCE results further confirm that the DSSC based on ZnO HD structures possesses an increased light-harvesting ability compared with the nanowire array DSSC. The increase is attributed to the special porous structure of the HD ZnO structures, which can absorb more dye molecules on the photoanode.

The effect of light intensity on the photovoltaic properties of the solar cell was also investigated. Figure 5a,b shows the variation of the photovoltaic properties for the annealed ZnO

HD nanostructured DSSC under different illumination intensities. The J_{sc} increased linearly with increasing light intensity, whereas the V_{oc} increases at lower intensity but saturates at higher intensity. The linear J_{sc} relationship with illuminated intensity indicates that a mass transport mechanism is not dominated in our DSSC.[27] The decrease of FF with increasing intensity could be due to the resistance increase of the DSSC under high-intensity illumination.[28] The exact reasons for the decrease of fill factors are not clear at the moment.

The improved photovoltaic performance of the HD ZnO DSSC can be attributed to the special morphologies of the HD ZnO structures. First, the porous feature of the HD ZnO offers a higher surface area for absorption of dye molecules, which is the key to achieving a higher current density. Meanwhile, the structures keep the one-dimensional feature and good crystallinity. These nanowires connect with each other to form a dense network, which can provide many transport channels to ensure rapid transportation of photoexcited electrons and, therefore, suppress the charge combination process. As a result, both the V_{oc} and the J_{sc} increase. Furthermore, the light-scattering effect may be another reason for the improved efficiency of the HD-ZnO DSSC. It has been reported that large particles added into the small nanoparticle film photoanode of DSSCs would improve the J_{sc} because the large particles could induce light scattering and increase optical path lengths.[29−31] In the present work, we believe that the ZnO HD structures can also induce light scattering and lead to more effective photon capturing because all of the nanowires in the ZnO HD structures grow in different directions. In addition, the ZnO HD structures consist of assembled porous ZnO nanowires and the whole structures can act as the scattering centers in the photoanode. This assumption was also exemplified by the observation that the HD ZnO films show a white color, whereas the ZnO nanowire array shows a semitransparent gray color.

4. Conclusions

ZnO HD nanostructures have been synthesized by a low-temperature hydrothermal method. The ZnO HD nanostructures consist of highly dense porous nanowires growing in six symmetric directions. The porous HD materials provide a possible route to further increase the surface area of one-dimensional materials. A DSSC based on these nanostructures shows an improved photovoltaic performance. An overall efficiency of 2.49% and IPCE of 60% at 520 nm were obtained under 1 sun illumination. The annealing treatment was also found to further improve the fill factor of the DSSC. These results suggested that the HD ZnO nanostructure is a promising material for application in DSSCs.

Acknowledgment. This work was supported by a grant from CityU (Project No. 7002295). The authors would also like to acknowledge support from the U.S. Army International Technology Center-Pacific, the National Basic Research Program of China (973 Program) (Grant Nos. 2007CB936000 and 2006CB933000), the National High Technology Research and Development Program of China (863 Program) (Grant Nos. 2006AA03Z302 and 2007AA03Z301), and the National Natural Science Foundation of China (Grant No. 60806028).

References and Notes

(1) Grätzel, M. *Nature* **2001**, *414*, 338.
(2) Kalyanasundaram, K.; Grätzel, M. *Coord. Chem. Rev.* **1998**, *77*, 347.
(3) Kuang, D.; Brillet, J.; Chen, P.; Takata, M.; Uchida, S.; Miura, H.; Sumioka, K.; Zakeeruddin, S. M.; Grätzel, M. *ACS Nano* **2008**, *2*, 1113.
(4) Regan, B. O.; Grätzel, M. *Nature* **1991**, *353*, 737.
(5) Stergiopoulos, T.; Arabatzis, I. M.; Cachet, H.; Falaras, P. *J. Photochem. Photobiol., A* **2003**, *155*, 163.
(6) Grätzel, M. *Inorg. Chem.* **2005**, *44*, 6841.
(7) Keis, K.; Magnusson, E.; Lindstrom, H.; Lindquist, S. E.; Hagfeldt, A. *Sol. Energy Mater. Sol. Cells* **2002**, *73*, 51.
(8) Tennakone, K.; Bandara, J.; Bandaranayake, P. K. M.; Kumara, G. R. A.; Konno, A. *Jpn. J. Appl. Phys.* **2001**, *40*, L732.
(9) Huang, S. Y.; Schlichthorl, G.; Nozik, A. J.; Grätzel, M.; Frank, A. J. *J. Phys. Chem. B* **1997**, *101*, 2576.
(10) Ito, S.; Liska, P.; Comte, P.; Charvet, R.; Pechy, P.; Bach, U.; Mende, L. S.; Zakeeruddin, S. M.; Kay, A.; Nazeeruddin, M. K.; Grätzel, M. *Chem. Commun.* **2005**, 4351.
(11) Law, M.; Greene, L. E.; Johnson, J. C.; Saykally, R.; Yang, P. D. *Nat. Mater.* **2005**, *4*, 455.
(12) Law, M.; Greene, L. E.; Radenovic, A.; Kuykendall, T.; Liphardt, J.; Yang, P. *J. Phys. Chem. B* **2006**, *110*, 22652.
(13) Snaith, H. J.; Mende, L. S. *Adv. Mater.* **2007**, *19*, 3187.
(14) Chuangchote, S.; Sagawa, T.; Yoshikawa, S. *Appl. Phys. Lett.* **2008**, *93*, 033310.
(15) Kamat, P. V. *J. Phys. Chem. C* **2007**, *111*, 2834.
(16) Martinson, A. B. F.; Hamann, T. W.; Pellin, M. J.; Hupp, J. T. *Chem.—Eur. J.* **2008**, *14*, 4458.
(17) Greene, L.; Yubas, B.; Law, M.; Yang, P. *Inorg. Chem.* **2006**, *45*, 7535.
(18) Martinson, A. B. F.; Elam, J. W.; Tupp, J. T.; Pellin, M. J. *Nano Lett.* **2007**, *7*, 2183.
(19) Zhu, J.; Peng, H. L.; Chan, C. K.; Jarausch, K.; Zhang, X. F.; Cui, Y. *Nano Lett.* **2007**, *7*, 1095.
(20) Wang, J. X.; Sun, X. W.; Wei, A.; Lei, Y.; Cai, X. P.; Li, C. M.; Dong, Z. L. *Appl. Phys. Lett.* **2006**, *88*, 233106.
(21) Jiang, C. Y.; Sun, X. W.; Lo, G. Q.; Kwong, D. L.; Wang, J. X. *Appl. Phys. Lett.* **2007**, *90*, 263501.
(22) Wang, J. X.; Sun, X. W.; Yang, Y.; Huang, H.; Lee, Y. C.; Tan, O. K.; Vayssieres, L. *Nanotechnology* **2006**, *17*, 4995.
(23) Sun, X. W.; Wang, J. X.; Wei, A. *J. Mater. Sci. Technol.* **2008**, *24*, 649.
(24) Vayssieres, L.; Keis, K.; Hagfeldt, A.; Lindquist, S. E. *Chem. Mater.* **2001**, *13*, 4395.
(25) Wei, A.; Sun, X. W.; Xu, C. X.; Dong, Z. L.; Yang, Y.; Tan, S. T.; Huang, W. *Nanotechnology* **2006**, *17*, 1740.
(26) Wang, J. X.; Sun, X. W.; Huang, H.; Lee, Y. C.; Tan, O. K.; Yu, M. B.; Lo, G. Q.; Kwong, D. L. *Appl. Phys. A: Mater. Sci. Process.* **2007**, *88*, 611.
(27) Hamann, T. W.; Martinson, A. B. F.; Elam, J. W.; Pellin, M. J.; Tupp, J. T. *Adv. Mater.* **2008**, *20*, 1560.
(28) Beek, W. J. E.; Wienk, M. M.; Janssen, R. A. J. *Adv. Funct. Mater.* **2006**, *16*, 1112.
(29) Nazeeruddin, M. K.; Pechy, P.; Renouard, T.; Zakeeruddin, S. M.; Baker, R. H.; Comte, P.; Liska, P.; Cevey, L.; Costa, E.; Shklover, V.; Spiccia, L.; Deacon, G. B.; Bignozzi, C. A.; Grätzel, M. *J. Am. Chem. Soc.* **2001**, *123*, 1613.
(30) Zhang, Q. F.; Chou, T. P.; Russo, B.; Jenekhe, S. A.; Cao, G. Z. *Angew. Chem., Int. Ed.* **2008**, *47*, 2402.
(31) Barbe, C. J.; Arendse, F.; Comte, P.; Jirousek, M.; Lenzmann, F.; Shklover, V.; Grätzel, M. *J. Am. Ceram. Soc.* **1997**, *80*, 3157.

JP100637C